JOURNAL OF FOOD QUALITY & HAZARDS CONTROL
SHAHID SADOUGHI UNIVERSITY OF MEDICAL SCIENCES & HEALTH SERVICES

Journal of Food Quality and Hazards Control 13 (2026) 109-20

Development of a Novel Antimicrobial Active Surface via Integration of tetracycline within an Acrylate Coating and Soluble Soybean Polysaccharide Matrix

D. Salarbashi [1,2], M. Tafaghodi [3,4], S.A. Mohajeri [5], B. Jafari [6], M. Saghravanian [7], F. Hadizadeh [8], B.S. Fazly Bazzaz [8,9], L. Ansari [10], S. Tafazzoli Mehrjardi [11], Jamal Al-Sabahi [12 *], U.H. Al Hoqani [13]

1. Department of Nutrition, Food Science and Clinical Biochemistry, School of Medicine, Gonabad University of Medical Sciences, Gonabad, Iran
2. Clinical Research Development Unit, Imam Reza Hospital, Faculty of Medicine, Mashhad University of Medical Sciences, Mashhad, Iran
3. Nanotechnology Research Center, Pharmaceutical Technology Institute, Mashhad University of Medical Sciences, Mashhad, Iran
4. Pharmaceutics Department, School of Pharmacy, Mashhad University of Medical Sciences, Mashhad, Iran
5. Pharmaceutical Research Center, Pharmaceutical Technology Institute, Mashhad University of Medical Sciences, Mashhad, Iran
6. Sustainable Membrane Technology Research Group, Department of Chemical Engineering, Faculty of Petroleum, Gas and Petrochemical Engineering, Persian Gulf University, 75169, Bushehr, Iran
7. Department of Chemistry, Mashhad Branch, Islamic Azad University, Mashhad, Iran
8. Biotechnology Research Center, Pharmaceutical Technology Institute, Mashhad University of Medical Sciences, Mashhad, Iran
9. Pharmaceutical Control Department, School of Pharmacy, Mashhad University of Medical Sciences, Mashhad, Iran
10. Cellular and molecular research center, cellular and molecular medicine research institute, Urmia university of medical sciences, Urmia, Iran
11. Pharmaceutics Department, School of Pharmacy, Mashhad University of Medical Sciences, Mashhad, Iran
12. Central Instrumentation Laboratory, College of Agricultural and Marine Sciences, Sultan Qaboos University, Oman
13. Applied Sciences Department, College of Applied Sciences and Pharmacy, University of Technology and Applied Sciences, Muscat, Oman

HIGHLIGHTS

- A bilayer antimicrobial surface was developed by applying a tetracycline-loaded acrylate coating onto plasma-treated SSPS/nanoclay film.
- Sustained tetracycline release achieved complete elimination of *staphylococcus aureus* after 24 h in time-kill assays.
- Nanoclay addition (up to 10 wt %) significantly enhanced storage modulus and glass transition temperature of the nanocomposite.
- Successful bilayer formation was confirmed through SEM, FT-IR, and XRD analyses without phase separation.

Article type
Original article

Keywords
Decontamination
Plasma Gases
Anti-Bacterial Agents
Tetracycline
Surface Properties

Article history
Received: 1 Dec 2025
Revised: 26 Jun 2026
Accepted: 28 Jun 2026

ABSTRACT

Background: The proliferation of harmful germs on surfaces necessitates the development of active, self-decontaminating materials. This study aims to develop a novel antimicrobial active surface.

Methods: A double-layer bionanocomposite was fabricated. The base layer was a film of Soluble Soybean Polysaccharide (SSPS) and nanoclay Na^+ . Using Molecularly Imprinted Polymer (MIP) technology, tetracycline was integrated into an acrylate coating, which was then applied to the polysaccharide film via oxygen plasma treatment to form the active top layer. The composite was characterized using Fourier Transform Infrared Spectroscopy (FT-IR), X-Ray Diffraction (XRD), Scanning Electron Microscopy (SEM), Transmission Electron Microscopy (TEM), and dynamic

*Corresponding author (J. Al-Sabahi)
E-mail: jamal@squ.edu.om
ORCID ID: https://orcid.org/0000-0002-2244-5292

To cite: Salarbashi, D., Tafaghodi, M., Mohajeri, S.A., Jafari, B., Saghravanian, M., Hadizadeh, F., et al. (2026) 'Development of a novel antimicrobial active surface via integration of tetracycline within an acrylate coating and soluble soybean polysaccharide matrix', *Journal of Food Quality and Hazards Control*, 13(2), pp. 109-20.

DOI: 10.18502/jfqhc.13.2.22140 Journal website: http://jfqhc.ssu.ac.ir

mechanical analysis. Its antibacterial activity against *Staphylococcus aureus* was evaluated through a time-kill study over 24 h. All experiments were performed in triplicate (n=3). Statistical analysis was conducted using ANOVA followed by Duncan's multiple range test

Results: Spectroscopy confirmed the integration of components. Morphological analyses showed a uniform, defect-free bilayer structure with strong interfacial adhesion. The incorporation of nanoclay significantly improved the mechanical properties, increasing the storage modulus and Glass Transition Temperature (Tg). Time-kill assays demonstrated a sustained release of tetracycline, leading to a bacteriostatic effect and a complete eradication of *Staphylococcus aureus* after 24 h.

Conclusion: The developed bilayer composite successfully functions as an active surface with prolonged self-decontaminating properties, achieved through the sustained release of tetracycline. This promising material can inhibit microbial growth on surfaces, potentially extending the shelf-life of products.

Abbreviations
AIBN=Azobisisobutyronitrile
CFU=Colony Forming Unit
EGDMA=Ethylene Glycol Dimethacrylate
ENPs=Engineered Nanoparticles
FT-IR=Fourier Transform Infrared Spectroscopy
HEMA=Hydroxyethyl Methacrylate
MAA=Methacrylic Acid
MIP=Molecularly Imprinted Polymer
MMT=Montmorillonite
NIP=Non-Imprinted Polymer
PAA= Poly Acrylic Acid
SEM=Scanning Electron Microscope
SSPS=Soluble Soybean Polysaccharide
TEM=Transmission Electron Microscopy
Tg=Glass Transition Temperature
XRD=X ray-Diffraction

Introduction

Surface contamination by pathogenic microorganisms has become a major concern for human well-being, particularly among the younger population (Abdolshahi *et al.*, 2022). Consequently, considerable efforts have been devoted to develop active antimicrobial surfaces to incorporate antimicrobial compounds (such as antioxidants and antimicrobial compounds) on active surfaces (with the ability to carry these compounds) to eliminate these adverse conditions (Altiok, Altiok and Tihminlioglu, 2010; Sevimli and Yılmaz, 2012). Active antimicrobial surfaces have recently emerged as an effective strategy in which it focuses on a functional surface to protect products and objects such as packaging, children's toys, hospital supplies and surgical equipment against pathogenic microorganisms. An active surface can be obtained by adsorbing an active compound on the surface through ionic and/or covalent bonding and then slowly releasing them into the environment (Monjazeb Marvdashti *et al.*, 2020). Among these approaches, Molecular Imprinting (MIP) technology has attracted increasing attention (Kioomars *et al.*, 2017). However, few studies have been conducted on this technology and it is still a developing technology.

Numerous polymers were used to make active surfaces (Primc and Mozetič, 2024). Among them, Soluble Soybean Polysaccharide (SSPS), is a biodegradable polysaccharide polymer that has properties such as low molecular weight and high solubility in water (Shaili, Abdorreza and Fariborz, 2015). However, this polymer alone has physical limitations in its structure to build an active surface, which can be addressed by nanotechnology (Fathi, Emam-Djomeh and Aliabbasi, 2021).

Today, Engineered Nanoparticles (ENPs) can be used to develop active surfaces, and the science of nanotechnology has made this possible for researchers (Heydari-Majd *et al.*, 2020). Among the ENPs, layered silicate i.e., Montmorillonite (MMT) has a high surface area and platy structure including two silica tetrahedral sheets fused to an edge-shared alumina octahedral. The unique properties of MMT, such as their commercial availability, low cost and relatively simple processability have led to their widespread use in the development of films and nanofibers (Salarbashi *et al.*, 2017).The addition of MMT to the biopolymer structure has also improved its antimicrobial, mechanical, thermal and barrier properties. Previous studies have shown that the application of ENPs improved the physicochemical properties of SSPS (Salarbashi *et al.*, 2017; Salarbashi and Tafaghodi, 2018; Salarbashi, Tafaghodi and Bazzaz, 2018; Salarbashi *et al.*, 2018).

Nowadays, various antimicrobial active compounds such as essential oils, bacteriocins, etc. are used to attach to antimicrobial active surfaces (Salarbashi, Tafaghodi and Heydari-Majd, 2020). Among them, tetracycline is a member of the family of broad-spectrum antibiotics that is widely used to treat infections, diseases, as well as a food preservative for animal growth promotion (Chen *et al.*, 2022).

Tetracycline also has important properties including reactive oxygen species scavenging, anti-apoptotic and anti-inflammatory effects. The antimicrobial properties of tetracycline, like those of other antibiotics, are due to its

[DOI: 10.18502/jfqhc.13.2.22140]

binding to bacterial ribosomes and impaired protein synthesis (He, Kai and Ding, 2011).

Since the slow-release rate of tetracycline is intended for residual antimicrobial activity over time, embedding it on an active surface can meet this strategy. There are several reasons why tetracycline is used as a potent antimicrobial to activate surfaces. First, tetracycline is active against a wide range of pathogens such as gram-negative and gram-positive bacteria, mycoplasmas, chlamydia, and rickettsia. Secondly, tetracycline has less toxicity and less moisture degradation than other members of the family (such as doxycycline, minocycline, oxytetracycline, etc.). Also, it can maintain its biological properties against gamma rays up to 32.4 kg of radiation. Third, the degradation temperature of tetracycline is about 70 °C for 24 h, and since active surfaces are used at ambient temperature, no degradation will be observed in the structure of tetracycline. Xia *et al.* (2015) developed an ampicillin□loaded acrylate coating on clay□modified polypropylene. However, their system did not use MIP, did not include an SSPS/nanoclay base layer, and was a single□layer coating. In contrast, tetracycline (a different antibiotic with broader clinical relevance) was selected, MIP technology was employed to achieve sustained release, and a bilayer structure consisting of an SSPS/nanoclay base film and a tetracycline-loaded acrylate coating was fabricated using oxygen plasma treatment. In another work, Czerwińska-Główka *et al.* (2021) incorporated tetracycline into a PEDOT coating. That study also employed a single layer (no SSPS, no nanoclay), did not use MIP, and relied on electrochemical polymerization rather than plasma□assisted bilayer assembly. A bilayer structure was designed to provide a physical barrier that further controls drug diffusion, a feature absent in the previously reported single-layer coating. The present study is the first to combine this specific SSPS/nanoclay base layer with a tetracycline-loaded MIP acrylate top layer.

To the best of the authors' knowledge, there is still no research dealing with the synthesis of embedded tetracycline in an acrylate coating and SSPS/nanoclay Na+-based bionanocomposite. The primary objective of this study is to develop a tetracycline-loaded bilayer active surface capable of sustained antimicrobial activity. Sustained release is the core innovation, as it enables prolonged self-decontamination. Structural enhancement (by incorporating nanoclay into the SSPS base layer) serves as a secondary objective to improve the mechanical and thermal properties of the film, ensuring its practical durability. Antibacterial optimization (complete kill of *S. aureus* within 24 h) is the functional outcome of the sustained release design. Thus, the three aims are not co-equal; sustained release is the principal goal, supported by structural reinforcement and validated by antibacterial efficacy.

Materials and methods

Materials

The SSPS was purchased from Fuji Oil Company (Osaka, Japan). The bacterial strain used in this study was *S. aureus* (PTCC No. 1112, equivalent to ATCC 6538P), a standard reference strain for antimicrobial susceptibility testing. The remaining chemicals, including glycerol, MMT, Methacrylic Acid (MAA), tetracycline, azobisisobutyronitrile (AIBN), ethylene glycol dimethacrylate (EGDMA), and Hydroxyethyl Methacrylate (HEMA), were purchased from Sigma-Aldrich (Merck, Germany).

SSPS/nanoclay Na+ film formation

SSPS/nanoclay Na^+ films were prepared using a modified solvent-casting method. Briefly, SSPS was dissolved in deionized water (0.016 g/ml) at a continuous stirring speed of 300 rpm at ambient temperature for 2 h. Subsequently, glycerol as a plasticizer was added into the solution and blended for another 2 h to yield a final plasticizer concentration of 50% w/w dry base. Subsequently, the dispersion containing 10% w/w dry base of MMT was distributed among the polysaccharide solution by homogenizing the mixture for 15 min at 13500 rpm, and then the dispersions were ultrasonicated for 5 min. Thereafter, the mixture was cast and air-dried at room temperature for 48 h. Finally, the dried films were peeled off carefully from the casting plate and pre-conditioned (RH 55%; 25 °C) in a desiccator for further assessments (Salarbashi *et al.*, 2017).

Fabrication of MIP and non-imprinted polymer (NIP)

MIP was prepared using the well-known imprinting technique. Briefly, tetracycline (5.68 mg) as the template and MAA (108 µl) as the functional monomer were dissolved in HEMA (2998 µl). The mixture was subsequently stirred for 15 min to promote interactions between tetracycline and MAA. AIBN (5.76 mg), as the initiator and EGDMA (160 mM), as the crosslinking agent, were then added to the aforementioned mixture and the sonication was continued for another 5-15 min. After that, the mixture was sparged with oxygen-free nitrogen for 2 min in an ice bath. Next, the obtained mixture was quickly poured into the desired polypropylene mold with 0.4 mm thickness and heated at 50-60 °C for 24 h to allow the radical polymerization to complete. Finally, the molded polymers were punched into 12 mm diameter disks and rinsed with distilled water for unreacted compound removal. Similarly, the same method was used to prepare

[DOI: 10.18502/jfqhc.13.2.22140]

the NIP without tetracycline (Xia *et al.*, 2015).

Fabrication of active coating

The active coating was prepared by applying the MIP polymer (synthesized as described in section 2.3) onto the SSPS/nanoclay Na^+ film. Prior to coating, the surface of the SSPS/nanoclay Na^+ film was pre-treated with oxygen plasma (Plasma Science PS500 RF, AST Products, Inc., Billerica, MA, USA) under the following conditions: power = 150 W, oxygen gas flow = 50 sccm, pressure = 0.5 Torr, treatment time = 4 s. This treatment was performed to improve interfacial adhesion between SSPS base layer and acrylate coating.

The MIP polymer mixture (containing tetracycline 5.68 mg, MAA 108 µl, HEMA 2998 µl, AIBN 5.76 mg, and EGDMA 160 mM, prepared as in section 2.3) was spread onto the plasma-treated SSPS/nanoclay film using an automatic film coater equipped with a spiral wire bar, producing a wet coating thickness of 0.4 mm. The coated film was then cured using a Fusion 300S UV light-curing conveyor (Fusion UV Systems Inc., Gaithersburg, MD, USA) at 1.8 kW power, 6-inch lamp, main wavelength 340 nm, for 4 s at room temperature (25±1 °C). After curing, the bilayer film (SSPS/nanoclay base + tetracycline-loaded MIP acrylate top layer) was stored in a desiccator at 25 °C and 55% relative humidity until further use. The same procedure was followed for NIP coating, except that tetracycline was omitted from the mixture (Xia *et al.*, 2015).

Characterization of SSPS/nanoclay Na+-based bionanocomposite

In this study, many characterization techniques were applied to identify the structural properties of the as-prepared nanocomposite. The X-Ray Diffraction (XRD) patterns were recorded in the 2θ range of 0°–40° with a scanning speed of 0.02° min^{-1} using X' Pert PW 3040/60 Philips diffractometer (Cu–Kα radiation (λ = 0.15478 nm), voltage 40 kV, current 30mA, Holland) (Zolfi *et al.*, 2015).

Chemical interactions within the nanocomposite were investigated using Fourier-Transform Infrared Spectroscopy (FT-IR). The KBr pellet of bionanocomposite film was subjected to analysis using an FT-IR spectrometer (Shimadzu, Japan) in the range of 400–4000 cm^{-1} (Shojaee-Aliabadi *et al.*, 2014).

The microstructure and cross-section morphology of films were examined using a Scanning Electron Microscope (SEM; LEO, Germany). In addition, the surface elemental composition was analyzed using an Energy Dispersive X-Ray Spectroscopy (EDX) system (Oxford, England) coupled with SEM. For cross-sectional imaging, the films were first broken in liquid nitrogen and then attached to a special grid. Subsequently, the grids were gold coated, and the fractured cross sections were imaged (Goldstein *et al.*, 2017).

Transmission Electron Microscopy (TEM) was used to examine the microstructure of nanoparticles. For this purpose, TEM images of nanoparticles and nanocomposites were obtained on a CM 120 Philips electron microscope (Philips, The Netherlands) and JEOL100 CXII TEM, respectively, at the Advanced Microscopic Research Center of Michigan State University School of Physics. To have a uniform and thin section of the nanocomposite before TEM analysis, CRX cryo ultramicrotome (RMC Boeckeler Instruments. Tucson, AZ) with a diamond knife at -120 °C was used. These samples must be imaged at low voltages, since they are sensitive to electron beams (Dhawan, 2025).

To study the dynamic-mechanical behavior of Soluble Soybean Polysaccharide-Polyacrylic Acid (SSPS-PAA), DMTA (DMA 2000 Tritec, England) was used. During DMTA analysis, the sample is subjected to a flexural, tensile, or torsional force. The sensitivity of this method to the determination of some transitions, like Glass Transition Temperature (Tg), is more than that of techniques such as DSC. During DMTA analysis, an oscillatory stress is applied to the sample, and the resulting strain is measured. For viscoelastic materials, the dynamic response consists of two components: a viscous part, which dissipates energy through molecular motion, and an elastic part, which stores energy until the stress is removed (Gnanasekaran, de With and Friedrich, 2018).

Antibacterial activity of SSPS embedded acrylate coating containing tetracycline

The antimicrobial activity was evaluated based on the ASTM E2149 standard method (ASTM International, 2001) with modifications regarding the test microorganism and exposure time. To evaluate the antibacterial efficacy of the tetracycline-loaded films, each film was immersed in a saline suspension of *S. aureus* at an initial concentration of 1×10^4 Colony Forming Unit [CFU]/ml. The films were then withdrawn at predetermined time points (0, 1, 3, and 24 h). The viable bacterial count remaining in the suspension was assessed using the pour plate technique. Serial ten-fold dilutions of the residual suspension were prepared, and 50 µl of each dilution was spread onto trypticase soy agar plates in triplicate. The plates were incubated at 37 °C for 18–24 h. The number of CFU was subsequently determined and compared with the initial bacterial concentration.

Determination of tetracycline loading content

The loading content of tetracycline in the MIP-coated film (SSPS-PAA containing tetracycline) was determined using the "wash-out" method. Five polymer discs (each

[DOI: 10.18502/jfqhc.13.2.22140]

with a diameter of 6 mm; total surface area of 5 discs = 141.3 mm²) were punched from the film using a punching machine. The discs were immersed in 2 ml of distilled water and stirred at room temperature for 1 h. The resulting solution was transferred to a 96-well microplate, and the absorption intensity was measured at the maximum wavelength of tetracycline (λ_max = 360 nm) using a microplate reader. The same washing procedure was repeated for five consecutive steps. After each wash, the concentration of tetracycline in the solution was calculated using a standard calibration curve with the line equation Y = 0.361X – 0.0768, where Y is the absorbance and X is the concentration (mg/ml). The percentage of drug removed in each step was determined relative to the total drug content.

Statistical analyses

Statistical analysis was conducted using SPSS 16.0 for Windows (SPSS Inc., Chicago, IL, USA). All experiments were performed in triplicate (n=3). Data were analyzed using one-way analysis of variance (ANOVA). At a p-value less than or equal to 0.05, the statistical differences were considered to be significant. Antimicrobial data were analyzed by Duncan's multiple range test. End results were considered as mean ± Standard Deviation (SD).

Results and discussion

Characterization of SSPS/nanoclay Na+-based bionanocomposite

-FT-IR analysis

FT-IR method was employed to identify the possible interactions between modified tetracycline imprinted polymer and the SSPS/nanoclay Na+ film. The appearance of all characteristic bands of naked acrylate (Ac) and tetracycline, SSPS, MMT, and nanocomposite were taken up in Figure 1 (a) to (g), respectively. For MMT, the absorbance peak observed at 1473 cm^{-1} corresponded to joining CH3–N. The two bands of average intensity absorption detected at 2929 and 2854 cm^{-1}, were attributed to –CH2 and –CH3, respectively. The broad peak situated at 3350 cm^{-1} corresponded to the vibration of O-H physisorbed by clay. The vibration of O-H of the silicated skeleton appeared at 3632 cm -1 (Hattab and Benharrats, 2015). For PAA, the absorption bands at 3449, 1727, and 848 cm^{-1} correlated to –NH stretching, C=O stretching, and C=C twisting of acrylate, respectively (Kunwong, Sumanochitraporn and Kaewpirom, 2011). The band at 2947 cm-1 denoted the C-H bond stretching vibration (Duan *et al.*, 2008). For SSPS, the stretching vibration of the O-H, C-H, and C-O groups appeared in the range of 3100-3500 cm^{-1}, 2850 to 3000 cm^{-1}, and 1100 cm^{-1}, respectively (Abdolshahi *et al.*; Bebu *et al.*, 2011; Abdolshahi *et al.*, 2020). Upon coating the SSPS film with tetracycline-containing acrylate, the broad O–H peak (3100–3500 cm^{-1}) showed a noticeable decrease in intensity, indicating partial involvement of the hydroxyl groups of SSPS in hydrogen bonding with the acrylate matrix and tetracycline.

When the SSPS film was coated in tetracycline acrylate, the intensity of the O-H peak slightly decreased which is ascribed to the reduction of concentration in the SSPS/tetracycline/MAA sample. No significant change was observed in the intensity of C-H peaks after coating SSPS (Figure 2 (B) and (C)). As shown in Figure 1, in SSPS/MMT/MAA the broad peak of the O-H group of SSPS disappeared; this can be attributed to more interactions between hydroxyl groups of the SSPS and MMT (Salarbashi *et al.*, 2014). This disappearance suggests strong interaction between hydroxyl groups of SSPS and silanol groups of MMT, leading to the formation of hydrogen bonds that restrict O–H stretching vibrations.

The bending vibrations of C-H in SSPS are situated in 1418 cm^{-1}. The peak at 1623 cm^{-1} indicated the presence of COO- groups. The peak at 1100 cm^{-1}, in which no change was observed with the addition of MMT or tetracycline, was assigned to the presence of glycoside bonds in the SSPS structure (Sherahi *et al.*, 2017).

The FT-IR spectra of pure tetracycline and the SSPS/tetracycline/MAA composite are presented in Figure 1. In the tetracycline spectrum, the stretching vibrations of N–H and O–H groups appeared as absorption bands between 3376 and 3306 cm^{-1}, while aromatic C–H stretching was observed in the region of 3112–2994 cm^{-1}. The peaks within 2932–2800 cm^{-1} and 1672–1585 cm^{-1} were attributed to CH_3 stretching and C=C stretching, respectively. Aromatic C–H bending was detected at 1453 cm^{-1}, and CH_3 bending gave a peak at 1360 cm^{-1}. The in-plane and out-of-plane deformation bands of the aromatic ring appeared in the ranges of 1232–1037 cm^{-1} and 684–500 cm^{-1}, respectively. Additionally, the C–N stretching vibration was observed at 996 cm^{-1} (Gunasekaran, Varadhan and Karunanidhi, 1996; Trivedi *et al.*, 2015).

Collectively, these spectral changes,-peak disappearance (O–H of SSPS/MMT), intensity reduction (O–H of SSPS after coating), and band shifting (C=O of acrylate), provided direct evidence of specific molecular interactions among SSPS, MMT, acrylate, and tetracycline, rather than simply confirming the presence of individual components.

[DOI: 10.18502/jfqhc.13.2.22140]

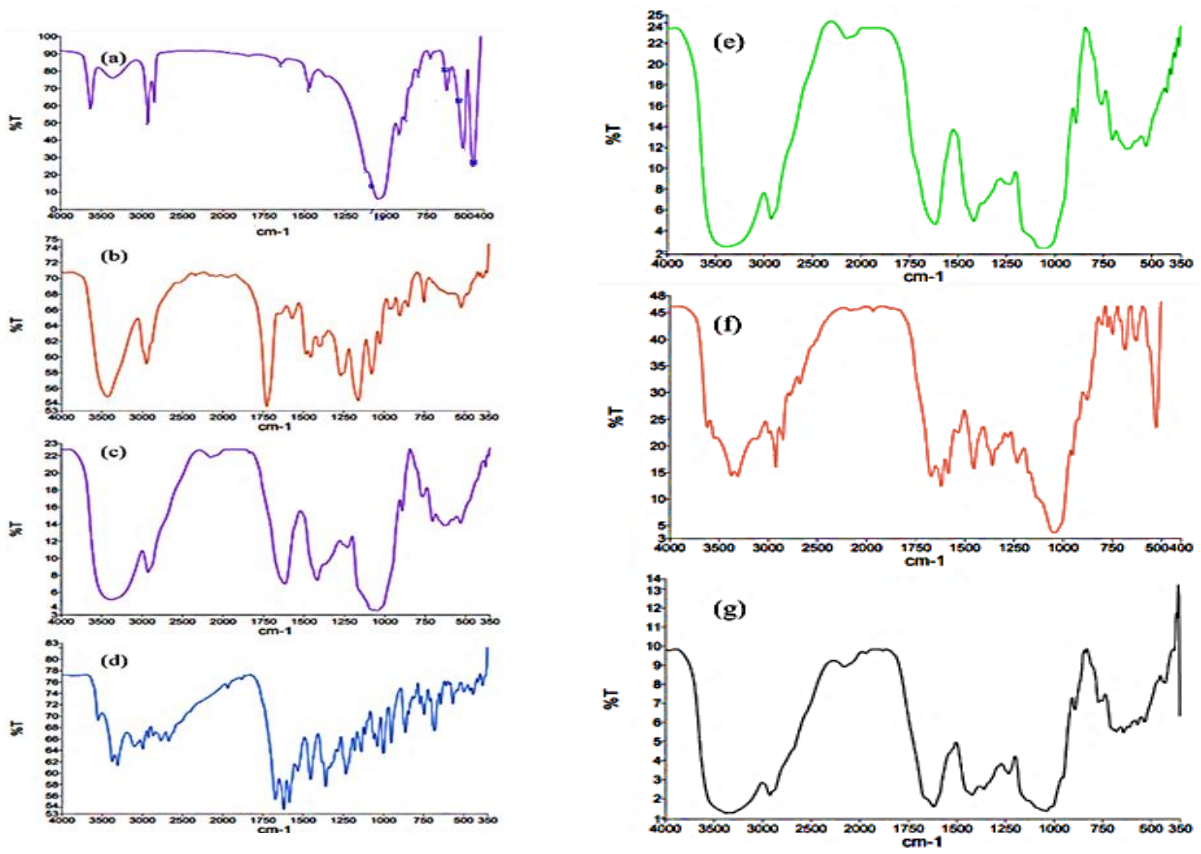

Figure 1: The Fourier-transform infrared spectroscopy spectra of (a) Montmorillonite (MMT), (b) Poly Acrylic Acid (PAA), (c) Soluble Soybean Polysaccharide (SSPS), (d) tetracycline, (e) SSPS + PAA, (f) MMT + SSPS + PAA, and (g) SSPS + PAA + tetracycline

Crystalline structure of the films

XRD test is used to evaluate the crystalline structure of components. The XRD patterns of the SSPS film, MMT, tetracycline, and SSPS-PAA film are illustrated in Figure 2. SSPS matrix showed a broad diffraction peak at 2θ = 20° (Figure 2) which is an indicator of the amorphous nature of SSPS (Xia *et al.*, 2015), consistent with studies on soybean soluble polysaccharides (Gao *et al*., 2022). There were several crystalline peaks in the MMT diffraction pattern at 2θ = 5.887, 19.891, 35.308, 40.416, 48.930, 54.233, 55.660, 61.799, 65.703, 73.329, 76.80° (Figure 2) (Fil, Özmetin and Korkmaz, 2014). Due to the amorphicity of SSPS, the intensity of MMT peaks decreased in the SSPS-MMT film (Figure 2). The position of SSPS peak (2θ=20°) remained almost unchanged. Therefore, it could be deduced that no chemical reaction occurred between SSPS and MMT. It also indicated successful physical dispersion of MMT layers in the SSPS matrix without chemical bonding. Similar results were reported by Kumar *et al*. (2023) for chitosan-MMT nanocomposites

PAA is amorphous; therefore, the diffraction pattern of this polymer shows an intense peak at 2θ values of 18.5 (Swain and Prusty, 2018). Besides, because of the crystalline nature of tetracycline, the intensity of SSPS/MMT/MAA peaks partly increased in the presence of this drug (wine peak compared to the cyan peak). Increased peak intensity in SSPS/MMT/MAA + tetracycline confirmed the drug crystalline nature.

[DOI: 10.18502/jfqhc.13.2.22140]

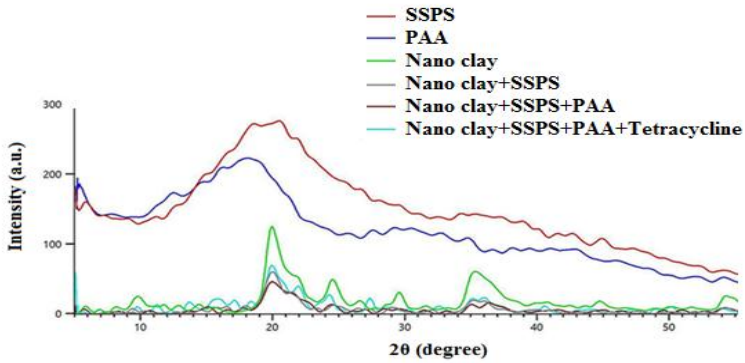

Figure 2: X-ray diffraction (XRD) patterns of neat SSPS (broad amorphous peak), pure tetracycline (sharp crystalline peaks), and the bilayer film (SSPS/montmorillonite [MMT] + tetracycline-PAA)
The bilayer retains the amorphous SSPS halo and shows reduced intensity of MMT peaks (e.g., at 2θ = 5.89°), indicating exfoliation.
PPA=Poly Acrylic Acid; SSPS=Soluble Soybean Polysaccharide

Morphological properties

The current study presents an experimental analysis of the nanoscale surface and the cross-section morphology of the neat and coated SSPS films by SEM (Figure 3 [a] and [b]). The surface image (Figure 3 [a]) of the SSPS showed a smooth and uniform layer without any holes or crevices. The absence of structural defects aligns with SSPS as an effective barrier material for food packaging applications. The amorphous nature of SSPS (confirmed by XRD) prevents grain boundary formation, resulting in uniform surfaces. This property is critical for minimizing moisture permeability in food packaging (Zhang *et al.*, 2023).

The coating of the tetracycline/acrylate layer on the SSPS film and preparation of a double layer was confirmed by the electron microscope image in Figure 3 (b). No phase separation or delamination at the interface suggests strong physical adhesion between layers.

The TEM image of nanoclay is shown in Figure 4. The aggregated structure of nanoparticles is observed. This aggregated structure is about 1000 nm.

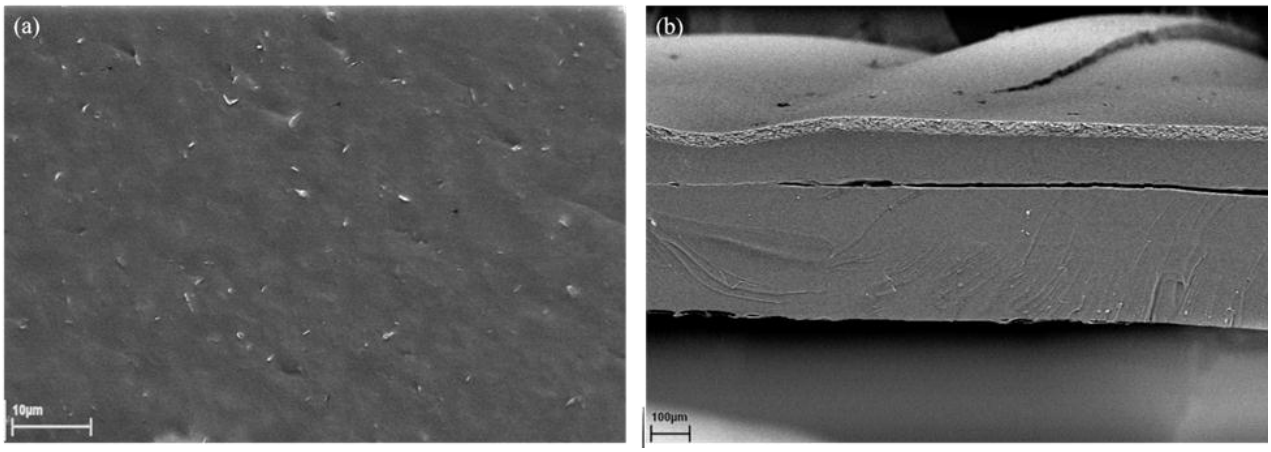

Figure 3: Scanning Electron Microscopy (SEM) images of (a) the neat Soluble Soybean Polysaccharide (SSPS) film and (b) the SSPS/Poly Acrylic Acid (PAA) film containing tetracycline

[DOI: 10.18502/jfqhc.13.2.22140]

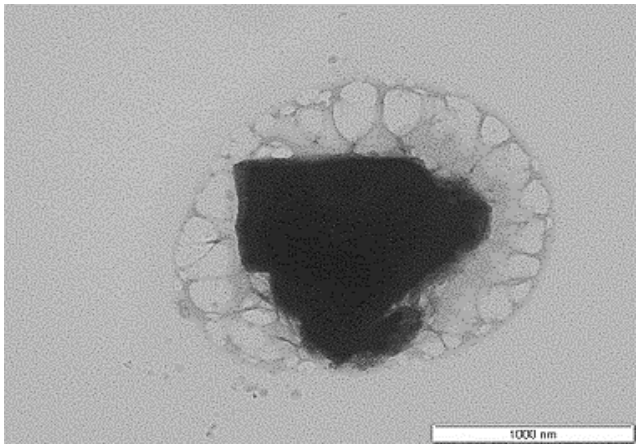

Figure 4: Transmission Electron Microscopy image of nanoclay

Dynamic mechanical characteristics

In a previous study (Salarbashi *et al.*, 2014), the results of dynamic-mechanical test of SSPS, acrylic, and SSPS-Ac, attached to each other using the plasma device, showed that at 100 °C the storage modulus of SSPS was 2.8 folds higher than PAA and was approximately in the middle of the neat SSPS and PAA for SSPS-PAA sample. As the temperature increased, the storage modulus of SSPS-PAA decreased with a mild slope which was ascribed to the good attachment of SSPS to Ac. In addition, in that study, it was shown that the glass temperature of the SSPS-PAA sample was -34 °C. Here, the present study investigated the storage modulus- and loss modulus- changes in the presence of different amounts of nanoclay.

With the addition of nanoclay, the storage modulus in the glass region increased, which was also reported by other researchers (Naveen Kumar *et al*., 2024). In this research, nanoclay was added to the SSPS matrix by weight percentages of 3, 7, and 10%. This increase is attributed to strong adhesion and interfacial interactions between the nanoparticles and polysaccharide matrix. Well-dispersed nanoclay acts as a physical crosslinker, restricting polymer chain mobility and enhancing rigidity (Alexandre and Dubois, 2000).

Figure 5 shows changes in the loss modulus in terms of temperature for SSPS-PAA and its nanoclay-loaded composites. The Tg is directly dependent on the movement of polymer chains and free volume in the polymer. At low temperatures, because the chains are compact and cannot move easily, free volume is neglected. As the temperature increases, the free volume in molecules increases and the main chains start to move in the amorphous region, which is called the Tg. Any factor that makes the polymer stiffer and hinders the movement of chains can increase the Tg. Adding nanoparticles to the polymer is a method that can be used to change the Tg (Vallés *et al.*, 2013). This trend aligns with Zabihi *et al*. (2011), who reported similar Tg increases in chitosan-clay nanocomposites. The magnitude of increase suggests effective nanoclay dispersion and strong polymer-particle interactions. However, excessive nanoclay loading can lead to agglomeration, reducing interfacial area and negating reinforcement (Bhattacharya, 2016).

If nanoparticles are well dispersed in polymer and linked to polymer throughstrong interactions, the Tg can increase. However, if there is an inappropriate distribution of these nanoparticles (for example due to the clumping of these nanoparticles), interfacial interactions can be reduced, which ultimately leads to a decrease in the Tg. Figure 5 (a) shows the temperature dependence of the storage modulus (E') of nanocomposites. It can be seen that the storage moduli of the nanocomposites were higher than those of the corresponding SSPS-PAA over the entire temperature range of the study (-100 °C to 150 °C). According to Figure 5 (b), it is clear that the Tg increases with the increase of nanoparticles up to 10% by weight. For example, by adding only 7 wt% of nanoclay, the Tg increases by 11 °C. On the other hand, it can be seen that by increasing nanoparticles content, the intensity of peaks and the area under the curve increase. This is likely due to the proper distribution of the nanoparticles, the lack of agglomeration, and the strong interactions between polymer and nanoparticles (Ahmadi *et al.*, 2012; Salarbashi *et al.*, 2017).

[DOI: 10.18502/jfqhc.13.2.22140]

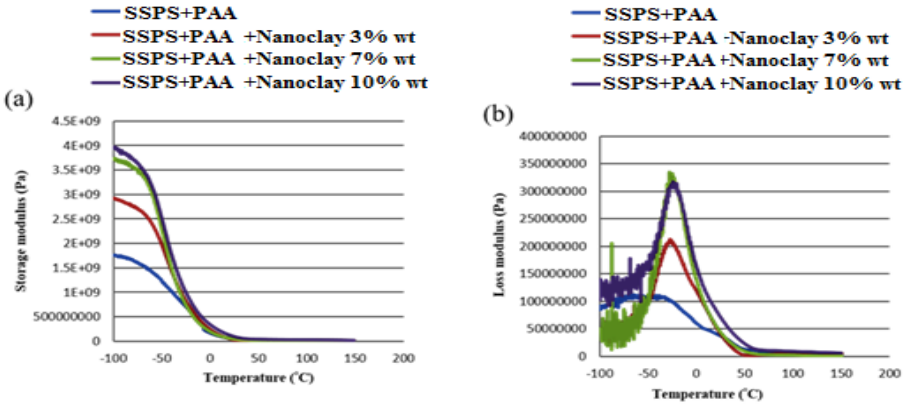

Figure 5: Variation of (a) storage modulus (E') and (b) loss modulus (E'') of SSPS-PAA nanocomposites with different nanoclay contents (0%, 3%, 7%, 10% w/w) at a frequency of 1 Hz. The Tg is marked by the peak in the loss modulus curve.
PPA=Poly Acrylic Acid; SSPS=Soluble Soybean Polysaccharide

Antimicrobial activity

Table 1 displays the antimicrobial efficacy of the tetracycline-loaded SSPS-PAA film as assessed through the time-kill assay. The grouping factor in this time-kill study was the exposure time (0, 1, 3, and 24 h). A one-way ANOVA was performed to assess the effect of exposure time on bacterial counts. The ANOVA revealed a significant effect of exposure time on bacterial viability ($F(3, 8) = 42.36$, $p<0.001$). Post-hoc pairwise comparisons were conducted using Duncan's multiple range test, and the results are presented in Table 1 (pairwise comparisons). Results showed that SSPS-PAA film containing Tetracycline after 1 h exposure in the suspension of *S. aureus* had no difference in the bacterial count with the original suspension. As exposure time continues (up to 3 h), a slight decrease (insignificant) in bacterial count is observed ($p>0.05$). However, after 24 h, the bacterial count reached about zero which showed a considerable difference with time 0, 1 h, and 3 h ($p<0.05$). Previous reports (Zheng *et al.*, 2024) attributed this phenomenon to the sustained release of the antibacterial compound, and the improvement of antibacterial activity and the shelf-life of foods, because of the delay in the growth of microorganisms on food surface. The acrylate-SSPS matrix acts as a diffusion barrier, delaying tetracycline release until hydration-triggered polymer swelling occurs.

Reports about the antibacterial activity of an active surface fabricated by embedded functionalized clays in an acrylate coating show the same findings (Xu and Charpentier, 2009, Xia *et al*. 2015, Bonilla *et al*., 2014). Table 1 indicates that the interaction between SSPS-PAA and tetracycline has no negative effect on antibacterial activity of tetracycline. In contrast, the interaction between amino groups of antibacterial agents and protein-based films can decrease the antibacterial activity. It is believed that these interactions can block the active sites by suppressing the desired antimicrobial reactions.

Table 1: Pairwise comparison of time-kill data for *Staphylococcus aureus* exposed to Polysaccharide-Polyacrylic Acid (SSPS-PAA) films containing tetracycline at various time points

Time (h) (I)	(J)	Mean Difference (I-J)	Std. Error (SE)	Sig.[a]	95% Confidence Interval for Difference [a]	
					Lower Bound	Upper Bound
0	1	5.000	11.547	0.707	-44.683	54.683
	3	41.667*	2.404	0.003	31.324	52.009
	24	63.667*	5.925	0.009	38.171	89.162
1	0	-5.000	11.547	0.707	-54.683	44.683
	3	36.667	13.383	0.111	-20.917	94.250
	24	58.667*	5.925	0.010	33.171	84.162
3	0	-41.667*	2.404	0.003	-52.009	-31.324
	1	-36.667	13.383	0.111	-94.250	20.917
	24	22.000	8.083	0.113	-12.778	56.778
24	0	-63.667*	5.925	0.009	-89.162	-38.171
	1	-58.667*	5.925	0.010	-84.162	-33.171
	3	-22.000	8.083	0.113	-56.778	12.778

The reported values are based on estimated marginal means.
a. Multiple comparison adjustment was performed using the Least Significant Difference method, which is equivalent to making no adjustment.
*The difference between means is statistically significant at $p<0.05$ level.

[DOI: 10.18502/jfqhc.13.2.22140]

Calculation of the loading content

The loading content of tetracycline in the MIP-coated film was determined as described in section 2.8. As shown in Table 2, approximately 70% of tetracycline was washed out in the first step, and after five washes the absorption intensity reached zero, indicating complete extraction of the drug. The total tetracycline content in 141.3 mm² of the film was calculated to be 31.8 mg. The detailed distribution of wash□out percentages and the statistical analysis (box plot, violin plot, and Pearson correlation) are presented in Figure 6. As illustrated in Figure 6A, the percentage of tetracycline removed decreased progressively from approximately 70% in the first wash to 1% in the fifth wash, indicating a rapid initial release followed by a sustained release profile. Figure 6B shows a strong negative Pearson correlation (r = -0.85) between washing step number and the amount of drug washed out, although the correlation was not statistically significant (p>0.05), likely due to the limited number of data points. The violin plot with kernel density estimation in Figure 6C reveals a bimodal distribution of washout data, suggesting two distinct release mechanisms: an initial burst release of surface-bound tetracycline and a slower diffusion-controlled release of drug embedded within the polymer matrix. These findings confirm that the MIP-coated film provides a sustained release profile, which is desirable for long-term antimicrobial activity.

Table 2: Changes in the amount of tetracycline at different stages of the leaching test

Washing step	Distilled water volume (ml)	Tetracycline washed out (mg)	Percent of wash out (%)
1	2	22.26±0.58 [a]	70
2	2	6.68±0.31 [b]	21
3	2	1.9±0.14 [c]	6
4	2	0.67±0.05 [d]	2
5	2	0.32±0.06 [e]	1
total	**10**	**31.8**	**100%**

The wash-out experiment was performed in triplicate (n=3). The values presented in Table 2 are the mean values of three independent measurements, with Standard Deviations (SD) less than 5% for each step

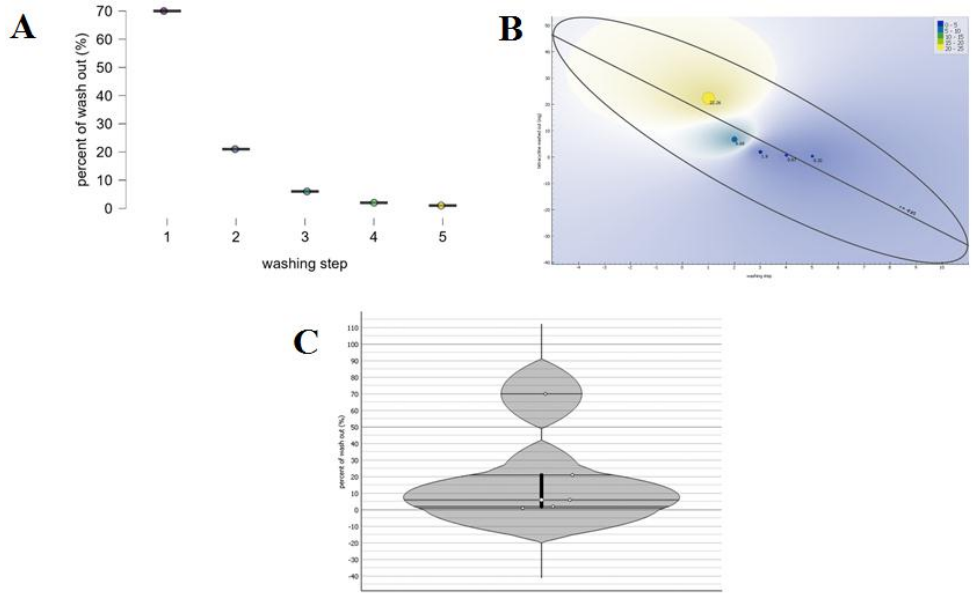

Figure 6: Statistical analysis of tetracycline washout from Molecularly Imprinted Polymer (MIP)-coated films over five sequential washing steps. (A) Box plot showing the percentage of tetracycline removed at each washing step. (B) Linear regression analysis of the relationship between washing step number and the amount of tetracycline washed out (mg). (C) Violin plot showing the distribution of tetracycline washout data

Conclusion

In this study, a novel double-layer antimicrobial active surface was successfully fabricated by integrating tetracycline into an acrylate coating via MIP technology and applying it onto an SSPS/nanoclay Na^+-based bionanocomposite film using oxygen plasma treatment. Structural characterization by FT-IR, XRD, SEM, and TEM confirmed the formation of a uniform, defect-free bilayer with strong interfacial adhesion and no phase separation. The incorporation of nanoclay (up to 10 wt%) significantly enhanced the mechanical properties, as evidenced by increased storage modulus and Tg (up to an 11 °C rise at 7 wt% nanoclay). The wash-out test revealed a sustained

[DOI: 10.18502/jfqhc.13.2.22140]

release profile of tetracycline, with approximately 70% of the drug released in the first wash followed by slower release, achieving a total loading content of 31.8 mg per 141.3 mm² of the film. The time-kill antibacterial assay against *S. aureus* demonstrated that tetracycline-loaded active surface achieved a bacteriostatic effect and complete bacterial elimination (reduction to zero CFU/ml) after 24 h of exposure. These findings confirm that the developed bilayer composite acts as an effective self-decontaminating surface with prolonged antimicrobial activity. Future studies are required to investigate the long-term performance, safety, and antimicrobial efficacy of the developed active surface against a broader range of microorganisms. In addition, optimization of the formulation and scalable fabrication should be explored for practical applications.

Author contributions

D.S. and M.T. conceptualized the study and designed the methodology; D.S, S.A.M., B.J., M.S., and F.H. conducted the experimental work and data acquisition; B.S.F.B. and L.A. performed the formal analysis and validation of data; S.T.M., J.A., and U.H.A.H. contributed to resources, supervision, and project administration; the original draft of the manuscript was written by D.S. and S.T.M. All authors participated in reviewing and editing the manuscript, provided critical intellectual feedback, read and approved the final version to be submitted, and agree to be accountable for all aspects of the study.

Acknowledgment

We sincerely appreciate Dr. Pankaj Sah for his valuable contributions in analyzing the data for this manuscript. His expertise and insightful input have significantly enhanced the quality of the present study. We are grateful for his support and collaboration.

Conflicts of interest

The authors declare that there is no conflict of interest.

Funding

This research received no specific grant from any funding agency in the public, commercial, or non-profit sectors.

Ethical consideration

Not applicable.

References

Abdolshahi, A., Heydari Majd, M., Abdollahi, M., Fatemizadeh, S. and Monjazeb Marvdashti, L. (2022) 'Edible film based on Lallemantia peltata L. seed gum: Development and characterization', *Journal of Chemical Health Risks*, 12(1), pp. 47-61. Available at: http://dx.doi.org/10.22034/jchr.2020.1896596.1118

Abdolshahi, A., Monjazeb Marvdashti, L., Salehi, B., Maggi, F. and Sharifi-Rad, J. (2020) 'Active packaging film based on lysozyme/polyvinyl alcohol/alyssum homalocarpum seeds gum', *Journal of Chemical Health Risks*, 10(4), pp. 261-275. Available at: https://doi.org/10.22034/jchr.2020.1890915.1091

Ahmadi, S., Manteghian, M., Kazemian, H., Rohani, S. and Darian, J.T. (2012) 'Synthesis of silver nano catalyst by gel-casting using response surface methodology', *Powder Technology*, 228, pp. 163-170. Available at: https://doi.org/10.1016/j.powtec.2012.05.012

Altiok, D., Altiok, E. and Tihminlioglu, F. (2010) 'Physical, antibacterial and antioxidant properties of chitosan films incorporated with thyme oil for potential wound healing applications', *Journal of Materials Science: Materials in Medicine*, 21, pp. 2227-2236. Available at: https://doi.org/10.1007/s10856-010-4065-x

ASTM International. (2001). ASTM E2149-01: Standard Test Method for Determining the Antimicrobial Activity of Immobilized Antimicrobial Agents Under Dynamic Contact Conditions. ASTM International, West Conshohocken, PA, USA. Available at: https://www.astm.org/e2149-01.html

Bebu, A., Szabó, L., Leopold, N., Berindean, C. and David, L. (2011) 'IR, Raman, SERS and DFT study of amoxicillin', *Journal of Molecular Structure*, 993(1-3), pp. 52-56. Available at: https://doi.org/10.1016/j.molstruc.2010.11.067

Chen, Y., Xia, Y., Liu, Y., Tang, Y., Zhao, F. and Zeng, B. (2022) 'Colorimetric and electrochemical detection platforms for tetracycline based on surface molecularly imprinted polyionic liquid on Mn3O4 nanozyme', *Biosensors and Bioelectronics*, 216, p. 114650. Available at: https://doi.org/10.1016/j.bios.2022.114650

Czerwińska-Główka, D., Przystaś, W., Zabłocka-Godlewska, E., Student, S., Cwalina, B., Łapkowski, M. and Krukiewicz, K. (2021) 'Electrically-responsive antimicrobial coatings based on a tetracycline-loaded poly (3, 4-ethylenedioxythiophene) matrix', *Materials Science and Engineering: C*, 123, p. 112017. Available at: https://doi.org/10.1016/j.msec.2021.112017

Dhawan, K. (2025) *Transmission Electron Microscopy Techniques*. Educohack Press.

Duan, G., Zhang, C., Li, A., Yang, X., Lu, L. and Wang, X. (2008) 'Preparation and characterization of mesoporous zirconia made by using a poly (methyl methacrylate) template', *Nanoscale research letters*, 3, pp. 118-122. Available at: https://doi.org/10.1007/s11671-008-9123-7

Fathi, M., Emam-Djomeh, Z. and Aliabbasi, N. (2021) 'Developing two new types of nanostructured vehicles to improve biological activity and functionality of curcumin', *Food Bioscience*, 44, p. 101386. Available at: https://doi.org/10.1016/j.fbio.2021.101386

Fil, B.A., Özmetin, C. and Korkmaz, M. (2014) 'Characterization and electrokinetic properties of montmorillonite', *Bulgarian Chemical Communications*, 46(2), pp. 258-263.

Gnanasekaran, K. de With, G. and Friedrich, H. (2018) 'Quantification and optimization of ADF-STEM image contrast for beam-sensitive materials', *Royal Society Open Science*, 5(5). Available at: https://doi.org/10.1098/rsos.171838

Goldstein, J.I., Newbury, D.E., Michael, J.R., Ritchie, N.W.M., Scott, J.H.J. and Joy, D.C. (2017) *Scanning electron microscopy and X-ray microanalysis*. Springer, New York, NY. Available at: https://doi.org/10.1007/978-1-4939-6676-9

[DOI: 10.18502/jfqhc.13.2.22140]

Gunasekaran, S., Varadhan, S.R. and Karunanidhi, N. (1996) 'Qualitative analysis on the infrared bands of tetracycline and ampicillin', *Proceedings-Indian National Science Academy Part A*, 62, pp. 309-316.

Hattab, Y. and Benharrats, N. (2015) 'Thermal stability and structural characteristics of PTHF–Mmt organophile nanocomposite', *Arabian Journal of Chemistry*, 8(3), pp. 285-292. Available at: https://doi.org/10.1016/j.arabjc.2011.03.010

He, X., Kai, T. and Ding, P. (2011) 'Heterojunction photocatalysts for degradation of the tetracycline antibiotic: a review', *Environmental Chemistry Letters*, 19(6), pp. 4563-4601. Available at: https://doi.org/10.1007/s10311-021-01295-8

Heydari-Majd, M., Ghanbarzadeh, B., Shahidi-Noghabi, M., Abdolshahi, A., Dahmardeh, S. and Malek Mohammadi, M. (2020) 'Poly (lactic acid)-based bionanocomposites: effects of ZnO nanoparticles and essential oils on physicochemical properties', *Polymer Bulletin*, 79, pp. 97-119. Available at: https://doi.org/10.1007/s00289-020-03490-z

Kioomars, S., Heidari, S., Malaekeh-Nikouei, B., Shayani Rad, M., Khameneh, B. and Mohajeri, S.A. (2017) 'Ciprofloxacin-imprinted hydrogels for drug sustained release in aqueous media', *Pharmaceutical Development and Technology*, 22(1), pp. 122-129. Available at: https://doi.org/10.1080/10837450.2016.1230131

Kunwong, D., Sumanochitraporn, N. and Kaewpirom, S. (2011) 'Curing behavior of a UV-curable coating based on urethane acrylate oligomer: the influence of reactive monomers', *Sonklanakarin Journal of Science and Technology*, 33(2), pp. 201-207.

Monjazeb Marvdashti, L., Abdulmajid Ayatollahi, S., Salehi, B., Sharifi- Rad, J., Abdolshahi, A., Sharifi-Rad, R. and Maggi, F. (2020) 'Optimization of edible Alyssum homalocarpum seed gum- chitosan coating formulation to improve the postharvest storage potential and quality of apricot (Prunus armeniaca L.)', *Journal of Food Safety*, 40(4), p. e12805. Available at: https://doi.org/10.1111/jfs.12805

Naveen Kumar, M., Vijaya Kumar, K.R., Suresh, G., Chinnathambi Muthukaruppan, M., Vezhavendhan, R., Chandramohan, P. and Rathinasabapathi, G. (2024) 'A study on: Impact on novel clay dispersion on mechanical, thermal and vibration properties of glass fiber-reinforced interpenetrating polymer networks (IPNs) hybrid composites', *Polymer Composites*. Available at: https://doi.org/10.1002/pc.28938

Primc, G. and Mozetič, M. (2024) 'Surface modification of polymers by plasma treatment for appropriate adhesion of coatings', *Materials*, 17(7), p. 1494. Available at: https://doi.org/10.3390/ma17071494

Salarbashi, D. and Tafaghodi, M. (2018) 'An update on physicochemical and functional properties of newly seed gums', *International Journal Of Biological Macromolecules*, 119, pp. 1240-1247. Available at: https://doi.org/10.1016/j.ijbiomac.2018.06.161

Salarbashi, D., Tafaghodi, M. and Bazzaz, B.S.F. (2018) 'Soluble soybean polysaccharide/TiO2 bionanocomposite film for food application', *Carbohydrate Polymers*, 186, pp. 384-393. Available at: https://doi.org/10.1016/j.carbpol.2017.12.081

Salarbashi, D., Tafaghodi, M., Bazzaz, B.S.F. and Jafari, B. (2018) 'Characterization of soluble soybean (SSPS) polysaccharide and development of eco-friendly SSPS/TiO2 nanoparticle bionanocomposites', *International Journal of Biological Macromolecules*, 112, pp. 852-861. Available at: https://doi.org/10.1016/j.ijbiomac.2018.01.182

Salarbashi, D., Tafaghodi, M. and Heydari-Majd, M. (2020) 'Fabrication of curcumin-loaded soluble soy bean polysaccharide/TiO2 nanoparticles bio-nanocomposite for improved antimicrobial activity', *Nanomed. Journal*, 7(4), pp.291-298. Available at: https://doi.org/10.22038/nmj.2020.07.00005

Salarbashi, D., Tajik, S., Shojaee-Aliabadi, S., Ghasemlou, M., Moayyed, H., Khaksar, R. and Noghabi, M.S. (2014) 'Development of new active packaging film made from a soluble soybean polysaccharide incorporated Zataria multiflora Boiss and Mentha pulegium essential oils', *Food Chemistry*, 146, pp. 614-622. Available at: https://doi.org/10.1016/j.foodchem.2013.09.014

Sevimli, F. and Yılmaz, A. (2012) 'Surface functionalization of SBA-15 particles for amoxicillin delivery', *Microporous and Mesoporous Materials*, 158, pp. 281-291. Available at: https://doi.org/10.1016/j.micromeso.2012.02.037

Shaili, T., Abdorreza, M.N. and Fariborz, N. (2015) 'Functional, thermal, and antimicrobial properties of soluble soybean polysaccharide biocomposites reinforced by nano TiO2', *Carbohydrate Polymers*, 134, pp. 726-731. Available at: https://doi.org/10.1016/j.carbpol.2015.08.073

Sherahi, M.H., Fathi, M., Zhandari, F., Hashemi, S.M.B. and Rashidi, A. (2017) 'Structural characterization and physicochemical properties of Descurainia sophia seed gum', *Food Hydrocolloids*, 66, pp. 82-89. Available at: https://doi.org/10.1016/j.foodhyd.2016.12.010

Shojaee-Aliabadi, S., Mohammadifar, M.A., Hosseini, H., Mohammadi, A., Ghasemlou, M., Hosseini, S.M., Haghshenas, M. and Khaksar, R. (2014) 'Characterization of nanobiocomposite kappa-carrageenan film with Zataria multiflora essential oil and nanoclay', *International Journal of Biological Macromolecules*, 69, pp. 282-289. Available at: https://doi.org/10.1016/j.ijbiomac.2014.05.015

Swain, S.K. and Prusty, K. (2018) 'Biomedical applications of acrylic-based nanohydrogels', *Journal of Materials Science*, 53, pp. 2303-2325. Available at: https://doi.org/10.1007/s10853-017-1726-x

Trivedi, M., Patil, S., Shettigar, H., Bairwa, K., Jana, S. and Bairwa, K. (2015) 'Spectroscopic characterization of chloramphenicol and tetracycline: An impact of biofield treatment', *Pharmaceutica Analytica Acta*, 6(7), pp. 2153-2435. Available at: https://doi.org/10.4172/2153-2435.1000395

Vallés, C., Kinloch, I.A., Young, R.J., Wilson, N.R. and Rourke, J.P. (2013) 'Graphene oxide and base-washed graphene oxide as reinforcements in PMMA nanocomposites', *Composites Science And Technology*, 88, pp. 158-164. Available at: https://doi.org/10.1016/j.compscitech.2013.08.030

Xia, Y., Ghasemlou, M., Rubino, M., Auras, R. and Baghdachi, J. (2015) 'Novel active surface prepared by embedded functionalized clays in an acrylate coating', *ACS Applied Materials and Interfaces*, 7(44), pp. 24944-24949. Available at: https://doi.org/ 10.1021/acsami.5b08579

Zheng, Y., Li, L., Shen, H., Chen, C. and Xie, J. (2024) 'Preparation of slow-release polylactic acid antibacterial active packaging films and its application in spinach preservation', *Food and Bioprocess Technology*, 18(2), pp. 1346-1364. Available at: https://doi.org/10.1007/s11947-024-03533-7

Zolfi, M., Khodaiyan, F., Mousavi, M. and Hashemi, M. (2015) 'Characterization of the new biodegradable WPI/clay nanocomposite films based on kefiran exopolysaccharide', *Journal of Food Science and Technology*, 52(6), pp. 3485-3493. Available at: https://doi.org/10.1007/s13197-014-1407-6

[DOI: 10.18502/jfqhc.13.2.22140]

